

# Observation and Analysis of Fracture Processes in Concrete with Acoustic Emission (AE) and Digital Image Correlation (DIC)

Gregor FISCHER \*, Jürgen BOHSE \*\*

\* Technical University of Denmark, Kgs. Lyngby, Denmark

\*\* BAM Bundesanstalt für Materialforschung und -prüfung, Berlin, Germany

**Abstract.** Fracture processes in concrete can be characterized by the formation of a Fracture Process Zone (FPZ), which is a region of the crack extending between the elastic region ahead of the crack tip over the crack bridging zone to the region where the crack opening is sufficiently large to prevent transfer of load across the crack faces. The formation of cracks and the development of the FPZ have typically been documented by Acoustic Emission (AE) methods and important conclusions regarding the nature of the FPZ and the propagation mechanisms of concrete have been drawn to form the basis of current fracture models for concrete.

The study presented in this paper focuses on Mode I cracking of concrete using compact tension specimens and is comparing the results of AE measurements to those obtained from documenting the cracking process by Digital Image Correlation (DIC). The findings from this comparison show that distinctly different AE events occur ahead of the crack tip, in the cementitious matrix at the crack tip and in the wake of the crack due to the increasing separation of the crack flanks and further opening of the crack. The DIC measurements indicate that crack initiation occurs with locally corresponding AE signals and furthermore suggest a continuous path of the crack from initiation to eventual transition to the stress-free zone. Based on these comparative measurements the study suggests that crack formation in unreinforced concrete is initiated by an individual, sharp microcrack rather than by a region of diffuse microcracking ahead of the eventual crack tip. Later on sharp crack branches originate from the main macrocrack path. Furthermore, the measurements with AE and DIC result in information on the nature of the deformation mechanisms occurring in distinct regions of the entire cracking process. AE signals detected using wideband sensors show quite different characteristics in time (waveform) and frequency (bandwidth) domain.

## 1. Introduction

Crack formation and propagation in concrete is governed by formation of a crack pattern and path due to the heterogeneity of the concrete microstructure and the presence of a stress field. Crack propagation in concrete has proven to be a complex phenomenon and the mechanisms behind concrete fracture have not yet been fully understood. Concrete fracture

is typically described by the concept of the fracture process zone (FPZ). The concept of the development of a FPZ is to a large extent based on acoustic emission techniques [1].

The description of concrete fracture has been repeatedly reassessed since the ground-breaking work on brittle fracture by Griffith [2]. Describing concrete fracture using linear elastic fracture mechanics is today known to be inappropriate due to the large extent of the FPZ in concrete. The problems associated with describing concrete fracture with Griffith's theory were believed to be accommodated by introducing cohesive models applied in non-linear plastic fracture mechanics, and thereby accommodating the issues associated with a large non-linear zone ahead of the crack tip [3], [4].

Although the models of Dugdale and Barenblatt still required the FPZ to be small, they provided inspiration to Hillerborg's Fictitious Crack Model [5] in which there are no restrictions to the length of the FPZ. Hillerborg's model was extended into the Crack Band Model by Bazant and Oh [6] in which the width of FPZ was accounted for. The basis of improving the fracture models of concrete has been the assumed existence and significance of the FPZ. It has been attempted by many authors to describe the FPZ and especially to determine the size of it and various measurement methods have been presented.

Today the most commonly applied method when investigating the FPZ is Acoustic Emission (AE) and the current understanding and modelling of the FPZ is to a large extent based on AE measurements. AE is a commonly used measurement technique for evaluation of the FPZ. There are a number of methods available for FPZ detection, but AE is described as one of the most promising methods [1]. By Otsuka and Date [7] AE is used for FPZ detection during an experiment similar to the one in the present paper. One of the advantages of AE is that cracking inside a specimen can be detected, whereas most other techniques only observe the specimen surface. However, in order to obtain reasonable accuracy the sensors must be placed in close proximity to the crack [1].

For damage classification often conventional features of AE signals or its correlation plots for identification of damage mechanisms are used, e.g. [8 – 10], however, their appropriateness for a clear and reliable separation of damage mechanisms has to be confirmed. Waveform features of AE signals (peak amplitude, rise time, duration) from the same source depend on material and wave propagation distance (attenuation and dispersion effects) [11]. The peak amplitude can be distance corrected and, hence, related to the source amplitude but amplitude distributions from different mechanisms often overlap each other. Other derived features like RA value (= rise time / peak amplitude) partially are not really meaningful because different source mechanisms can originate signals where rise times and peak amplitudes are correlated in a different way. Thereby damage mechanisms cannot be clearly separated.

The combination of Digital Image Correlation (DIC) and AE measurements for damage monitoring and characterization in fibre reinforced mortar was applied [12]. In this paper the new DIC technique is applied alongside with acoustic emission technique and the observations are compared to find out if additional information about the fracture mechanisms in concrete can be provided.

## **2. Experimental setup**

The objective of the experiments is to study crack formation in concrete and investigate the behaviour and influence of the FPZ. It is aimed to capture a crack as it propagates through the specimen and to study the AE activity near the crack tip as well as on a larger scale.

Concrete cracks are very likely to form in a complex and extensive pattern, which makes investigation of the crack tip complicated. To enable the investigation of a simpler crack pattern it is attempted to make a concrete test specimen that will form one isolated

crack. For the purpose of studying crack development, it is intended to propagate the crack in small increments. Each opening stage is to be observed by DIC, investigating if additional information on crack growth mechanisms can be obtained by DIC and/or by accompanying AE measurements.

### 2.1 Specimen geometry and loading

The specimens are cut from a concrete block of 500mm by 500mm by 600mm made by three concrete batches. The concrete is cured for 28 days in total with the first seven days of water curing. The concrete used in the experiments had a maximum aggregate size of 16mm with a cement content of 330kg/m<sup>3</sup> and had a self-compacting consistency. The trial cubes were tested after 28 days and the resulting compressive strength of the concrete was 65MPa.

In order to obtain uniform specimens for the investigation of the fracture process zone, all specimens were cut from the same concrete block. The block with cross section of 500mm by 500mm was cast with a recess of width 100mm and depth 50mm throughout the thickness of the block. After 28 days of curing the block was cut into slices of 25mm thickness.

A notch of length 150mm was cut from the recess towards the centre of the specimen to control the direction of the crack and to be able to anticipate the origin and the path of the crack. The notch is cut with a blade saw resulting in the notch having varying length over the specimen thickness. The single notch compact tension specimen is shown in Fig. 1 with the DIC observation areas indicated by the shaded rectangle and the six AE sensors attached around the DIC observation area. Manually introduced loading of the notch flanks causes crack propagation initiating at the tip of the notch and further opening of in the concrete in Mode I.

The loading was applied incrementally using a manual screw mechanism to ensure a stable load application and avoid a sudden propagation of the crack. The increase in CMOD was applied on average at 1.5µm per second. Images were taken at intervals of 5s and AE signals were constantly recorded.

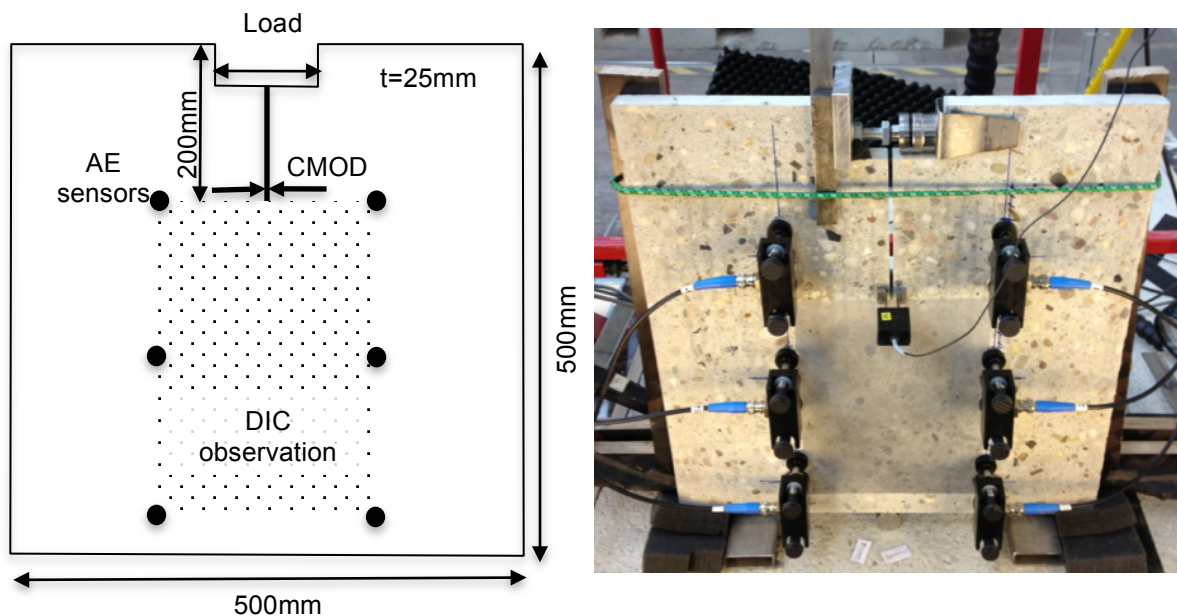


**Figure 1.** Experimental setup schematically (left) and specimen with fixed AE sensors, crack opening measurement (CMOD) and loading devices (right).

## 2.2 Digital Image Correlation (DIC) measurements

Photos are analyzed using DIC with the software Aramis (GOM Braunschweig, Germany). Series of images are processed and the displacement field of each stage is computed with reference to stage 0 which is the undeformed stage. The software creates a grid of rectangular shaped facets and computes the information in the four corners of each facet.

Throughout this study the chosen facet size is 15 pixels by 15 pixels with an overlap of 2 pixels which in this study corresponds to facets of approximately 200-300 $\mu\text{m}$ .

Aramis computes the displacement field by finding the same points in each image of the series, thus it must be able to recognize different points on the surface. In general a concrete surface may be too uniform for the software to distinguish between points on the surface. Typically surface contrast is applied by spray painting the surface slightly with two high contrast colors, e.g. white and black.

Below is shown an example of specimen 11\_01 using the image analysis software to visualize the deformations occurring at the specimen surface when subjected to increasing CMOD (Fig. 2). Here, the blue color indicates zero surface deformations (strain) and the changing colors of the spectrum up to red indicate areas of increasing deformations.

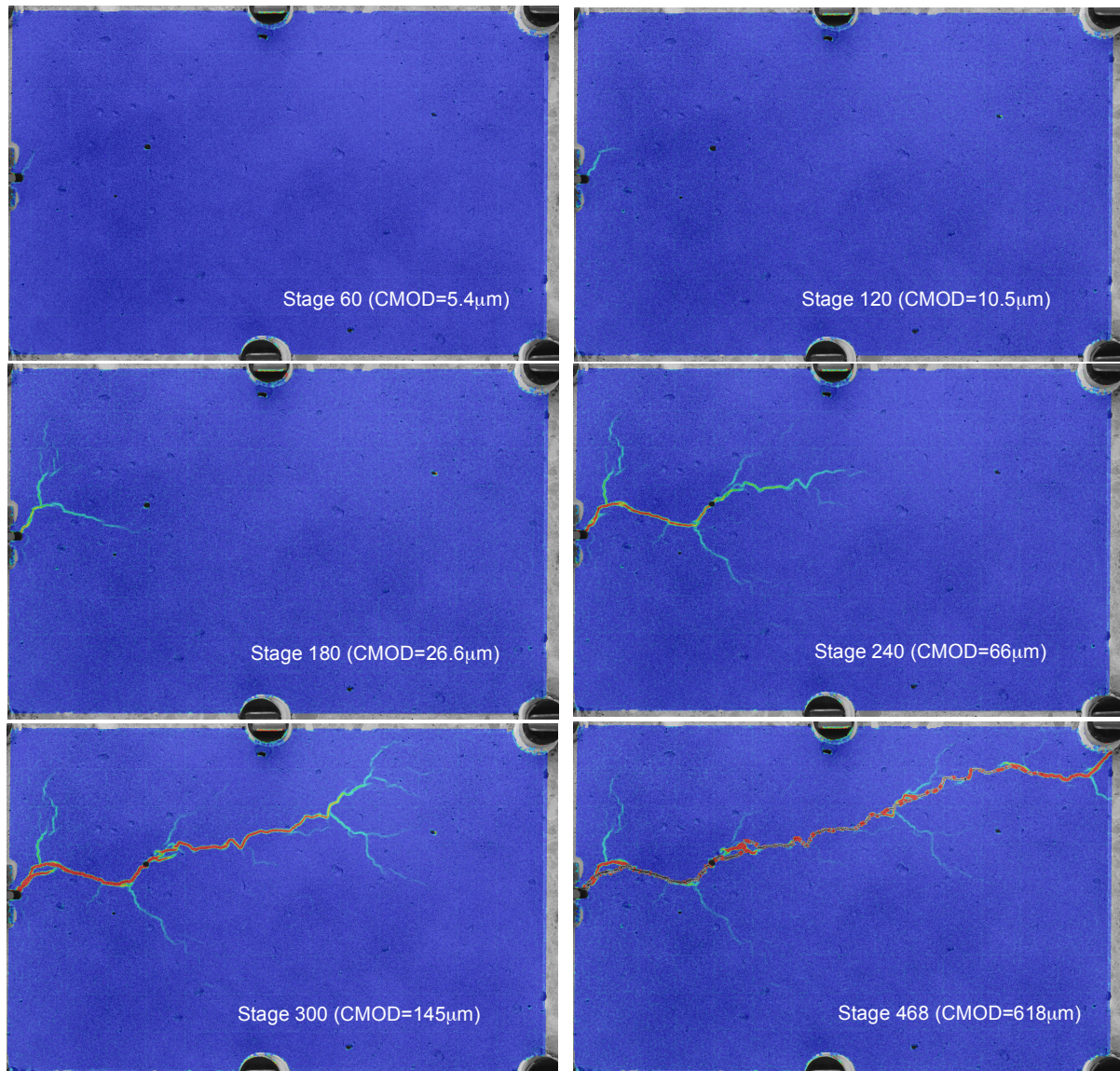


**Figure 2.** Process of crack formation in specimen 11\_01 indicating extent of cracking and CMOD corresponding to stages shown in Figure 5

### 2.3 Acoustic Emission (AE) measurements

AE measurements were performed using a MISTRAS system and wideband sensors type PAC-WD surrounding the DIC observation area to locate source events by 2D Planar (XY) location type. Parameters of AE measuring setup were: pre-amp. 40dB, detection threshold 34dB<sub>AE</sub>, analogue filter 20kHz...2MHz, sample rate 5MSPS and length 3k with 20 $\mu$ s pre-trigger for waveform recording.

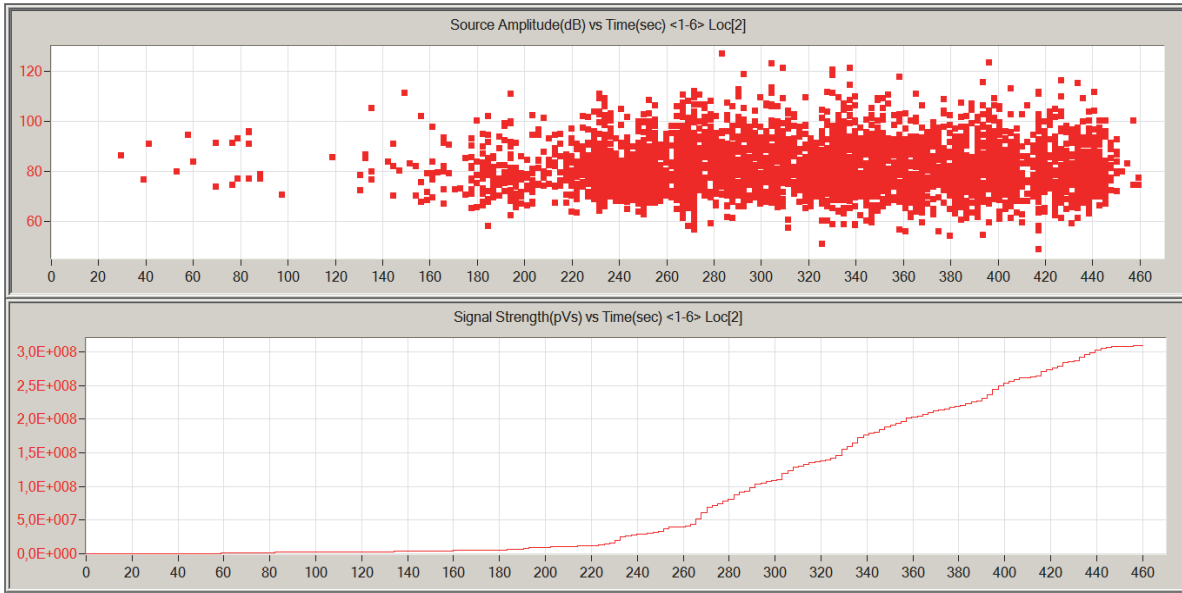


**Figure 3.** Distance corrected peak (source) amplitude (top) and cumulated signal strength energy of all located events (bottom) vs. test time up to stage 468 for specimen 11\_01 (see Figures 2 and 4).

The maximum source distance to the nearest AE sensor of the sensor array was 85mm. A high attenuation (20...30dB) in this near-field distance is observed. Measured attenuation curves were used for recalculation of signal peak amplitudes (Fig.3) at location of sources. On the other hand wave propagation of that distance causes some loss of signal power in the frequency range below 600kHz only.

## 3. Results and Discussion

### 3.1 Comparison of DIC and AE results

The load-CMOD relationship measured during the loading process using a conventional clip gage and a load cell are shown in Figure 4. It is apparent that crack initiation occurs rather discretely without signs of diffuse microcrack formation (Fig.5). Instead, the crack is attempting a number of different possible paths. Ultimately, the eventual macrocrack forms while the previously explored crack paths are not pursued further.

DIC measurement results of specimen 11\_01 show that first cracking appears at stage 60. This slight indication is intensified until stage 120 and increases further at subsequent stages.

Besides a few events between stages 80 and 90 AE measurement clearly indicate crack initiation by significant increase of acoustic emission activity and intensity of located AE events starting from stage 130 (see Fig. 6). Maybe more sophisticated location algorithms than those used here (2D Planar Location by 3 hits) could further enhance the location accuracy and achieve earlier detection of crack initiation, however, under laboratory test conditions only.

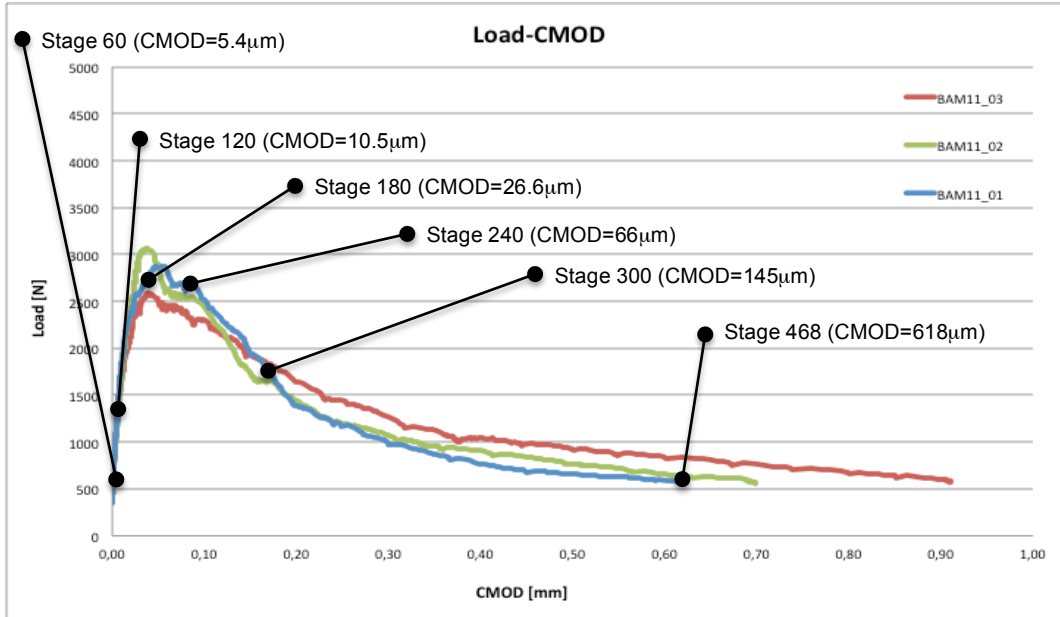


**Figure 4.** Load-CMOD relationship obtained for specimens 11\_01, 11\_02 and 11\_03. The CMOD for specimen 11\_01 are indicated in the graph



**Figure 5.** Overlay of DIC measurements and AE signals obtained up to CMOD = 145µm

### 3.2 Analysis of AE signals

AE signals from apparently different source mechanisms were located in distinct regions but at comparable source-sensor distance (i.e. similar influence of attenuation and dispersion effects) before crack initiation and during crack propagation. Waveform and frequency analysis results in three types/clusters of measured AE signals with quite different characteristics in both the time and frequency domain (Fig. 7):

Type 1: few “continuous”-like AE signals have long duration/rise times, weighted peak-frequencies  $f_{\text{weighted peak}} \approx 100 \dots 150 \text{ kHz}$  and source amplitudes  $A_{\text{source}} \leq 95 \text{ dB}_{\text{AE}}$

Type 2: most measured burst-type signals are characterized by shorter duration/rise times,  $f_{\text{weighted peak}} \approx 150 \dots 220 \text{ kHz}$  and  $A_{\text{source}} \leq 115 \text{ dB}_{\text{AE}}$

Type 3: a lower number of burst-type signals have shortest duration/rise times,  $f_{\text{weighted peak}} \approx 220 \dots 320 (\dots \approx 500) \text{ kHz}$  but of lower source amplitudes  $A_{\text{source}} \leq 105 \text{ dB}_{\text{AE}}$ .

The feature “weighted peak-frequency” was defined by Sause et al [12]

$$f_{\text{weighted peak}} = \sqrt{f_{\text{peak}} \cdot f_{\text{centroid}}}$$

and used for pattern recognition of AE from carbon fiber reinforced plastic specimens [13]. It smoothes the frequency information combining the peak and centroid frequencies and gives a good calculation of main power components in the spectrum of an AE signal.

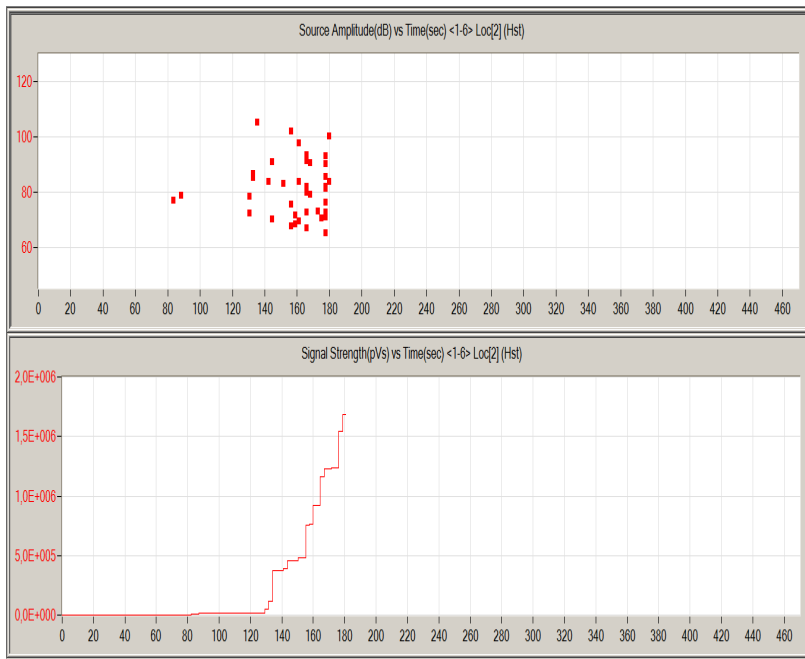


**Figure 6.** AE features from first events located in the area of crack initiation up to stage 180 for specimen 11\_01 (see Figures 2 and 4).

The above mentioned signal types can be interpreted as follows:

Type 1: Microscopic friction-like or shear pre-damage located at the transition of the elastic region into the FPZ ahead of the macrocrack tip. Those sources mark the paths of later macrocrack propagation and occurring crack branches along weak structural regions and/or areas of particularly high stress concentrations. The real mechanism is yet unclear for the authors.

Type 2 and 3: Those located events arise from

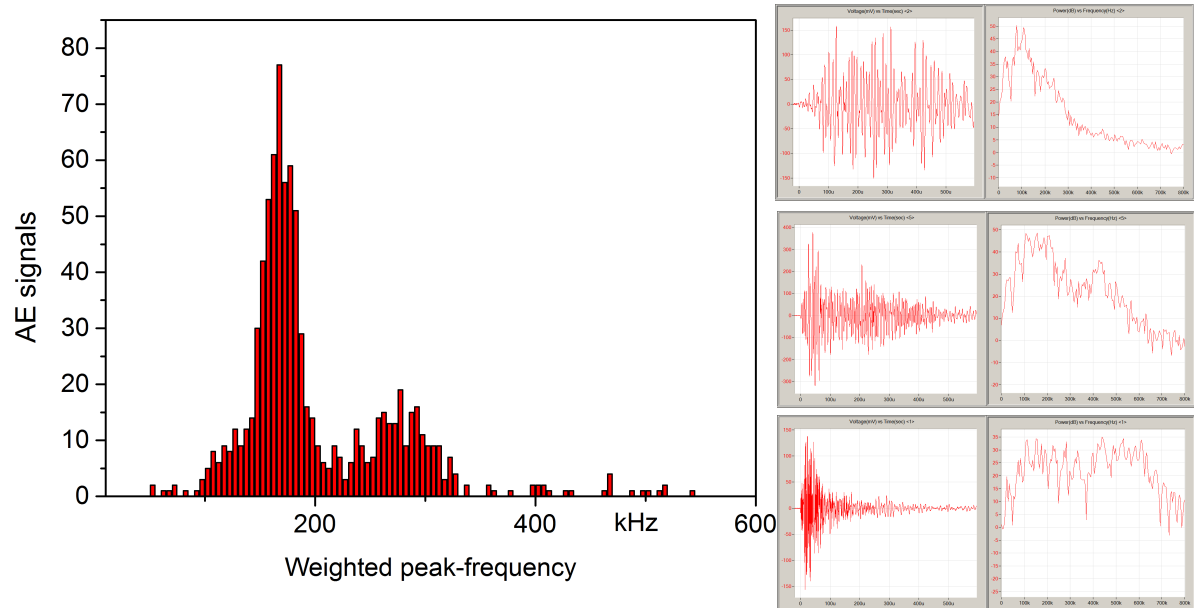


**Figure 7.** Weighted peak-frequency distribution of AE signals from located events in up to stage 240 shown in Figure 4 (left) and examples of waveforms/spectra for signal type 1, 2 and 3 (right, top to bottom).

the stages of crack opening and propagation. Thereby, measured burst signal amplitude is proportional to the involved area and velocity of source process. The bandwidth of signal is indirect proportional to the rise time of process.

#### 4. Conclusions

- The measurements with AE and DIC result in information on the nature of the deformation mechanisms occurring in distinct regions of the entire cracking process.
- Conclusions from comparison of DIC and AE results: The initiation of cracking and the subsequent opening of the crack is accompanied by distinctly different types of AE signals.
- Waveform and frequency analysis of AE signals from located events yields to three types/clusters of signals that can be correlated with microscopic damage at the transition of the elastic region into the FPZ ahead of the macrocrack tip (type 1) and events arise from the stages of opening or propagation of macrocrack and crack branches themselves (type 2 and 3).

#### Acknowledgement

The collaborative investigation between BAM and DTU described in this paper was established with support of BAM in the framework of a research visit of G. Fischer at BAM. The authors would like to acknowledge this support.

#### References

- [1] Shah, S. P. and Carpinteri, A. (1991). *Fracture Mechanics Test Methods for Concrete*. Chapman and Hall.
- [2] Griffith, A. A. (1921). The phenomena of rupture and flow in solids. *Philosophical Transactions of the Royal Society of London*, 221(1):163-198.
- [3] Dugdale, D. S. (1960). Yielding of steel sheets containing slits. *Journal of Mechanics and Physics of Solids*, 8(1):100\_104.
- [4] Barenblatt, G. I. (1962). The mathematical theory of equilibrium cracks in brittle fracture. *Advances in Applied Mechanics*, 7(1):55\_129.
- [5] Hillerborg, A., Mod er, M., and Petersson, P. E. (1976). Analysis of crack formation and crack growth in concrete by means of fracture mechanics and finite elements. *Cement Concrete Research*, 6(1):773\_782.
- [6] Bazant, Z. and Oh, B. (1983). Crack band theory for fracture of concrete. *Materials and Structures*, 16(93):155\_177.
- [7] Otsuka, K. and Date, H. (2000). Fracture process zone in concrete tension specimen. *Engineering Fracture Mechanics*, 65(1):111\_131.
- [8] Ohno, K, Ohtsu, M: Crack classification in concrete based on acoustic emission. *Construction and Building Materials* 24 (2010), 2339-2346
- [9] Vidya Sagar, R., Prasad, R.V., Rhagu Prasad, B.K., Rao, M.V.S.: Microcracking and Fracture Process in Cement Mortar and Concrete: A Comparative Study Using Acoustic Emission Technique. *Experimental Mechanics* 53 (2013), 1161-1175
- [10] Shahidan, S., Pulin, R., Bunnori, N., Holford, K.M.: Damage classification in reinforced concrete beams by acoustic emission signal analysis. *Construction and Building Materials* 45 (2013), 78-86
- [11] Aggelis, D.G., Mpalaskas, A.C., Ntalakas, D., Matikas, T.E.: Effect of wave distortion on acoustic emission characterization of cementitious materials. *Construction and Building Materials* 35 (2012), 183-190
- [12] Rouchier, S., Foray, G, Godin, N., Woloszyn, M., Roux, J.-J.: Damage monitoring in fibre reinforced mortar by combined digital image correlation and acoustic emission. *Construction and Building Materials* 38 (2013), 371-380
- [13] Sause, M.G.R., Gribov, A., Unwin, A.R., Horn, S.: Pattern recognition approach to identify natural clusters of acoustic emission signals. *Pattern Recognition Letters* 33:1 (2012), 17-23
- [14] Sause, M.G.R., Horn, S.: Simulation of acoustic emission in planar carbon fiber reinforced plastic specimens. *Journal of Nondestructive Evaluation* 29:2 (2010), 123-142